LAWRENCE
LIVERMORE
NATIONAL
LABORATORY

LLNL-JRNL-484435

Optical absorption in transparent conducting oxides: Mott transition or Mahan excitons?

A. Schleife, C. Rodl, F. Fuchs, K. Hannewald, F. Bechstedt

May 19, 2011

Physical Review Letters

Disclaimer

Optical absorption in transparent conducting oxides: Mott transition or Mahan excitons?

André Schleife,[1,2,3,*] Claudia Rödl,[1,2] Frank Fuchs,[1,2] Karsten Hannewald,[1,2] and Friedhelm Bechstedt[1,2]

[1] *Institut für Festkörpertheorie und -optik, Friedrich-Schiller-Universität, Max-Wien-Platz 1, 07743 Jena, Germany*
[2] *European Theoretical Spectroscopy Facility (ETSF)*
[3] *Condensed Matter and Materials Division, Lawrence Livermore National Laboratory, Livermore, CA 94550, USA*

(Dated: May 17, 2011)

Electron doping renders transparent oxides conductive although they have wide fundamental band gaps. The degenerate electron gas in the lowest conduction-band states of a doped oxide drastically modifies the Coulomb interaction between the electrons and, hence, the optical properties close to the absorption edge. We describe these effects by developing an *ab-initio* technique which captures highly interesting phenomena such as the Pauli blocking and the Fermi-edge singularity at the optical absorption onset, that occur in addition to quasiparticle and excitonic effects. We answer the question whether free carriers induce an excitonic Mott transition or trigger the evolution of Wannier-Mott excitons into Mahan excitons for the prototypical *n*-type ZnO.

PACS numbers: 71.10.Ca, 71.35.-y, 74.62.Dh, 78.20.Bh, 78.40Fy
Keywords: transparent conducting oxides, free carriers, Mahan exciton, Pauli blocking, Burstein-Moss shift

The important field of semiconductor optoelectronics is expected to continue its rapid growth in the future, driven, for instance, by the demand for highly efficient photovoltaics [1] and the next generation of displays [2]. In this context, oxide materials take a leading role [3] due to their impact for green-energy [4], intelligent-materials [5], or flexible-electronics [6] applications. In particular, the *transparent conducting oxides* (TCOs) rise hopes for cutting-edge applications because they are transparent in the visible spectral range (due to their large fundamental band gaps) as well as conductive (due to intentional or unintentional *n*-doping). While the TCOs comprise many compounds, one example which is especially interesting is zinc oxide (ZnO), since it is abundant in nature, cheap, as well as biocompatible. Due to a wealth of experimental results it is an ideal test bed for this work. ZnO has a band gap of 3.4 eV [7], a large exciton binding energy of about 60 meV [8], and can easily be *n*-doped [7].

A free electron gas resides in the lowest conduction band (CB) of an *n*-doped TCO [9], but also for nominally *undoped* ZnO electron concentrations as large as $n \approx 10^{17}$ cm^{-3} have been reported [7]. The effect of these free carriers on the optical properties is widely unknown; however, dramatic changes are expected in the spectral region which is most interesting for applications—the absorption edge. For undoped wurtzite (*wz*)-ZnO, experiment [8] and theory [10] consistently describe Wannier-Mott (WM)-like excitonic states [11] dominating the absorption below the fundamental band gap. They are caused by the Coulomb attraction between electrons and holes which stabilizes excited electron-hole pairs.

However, in an *n*-type system a photo-induced electron-hole pair also interacts with the degenerate electron gas in the CB [12]. The screening of the electron-hole attraction is significantly increased by the free carriers. This has originally been investigated merely for metals [13] or two-dimensional electron gases in quantum wells [14, 15]. Only recently it is becoming the focus of experimental studies for semiconductors such as the oxides [9], but also for the technologically equally important nitrides [16] and arsenides [17].

For highly doped semiconductors, the occurrence of an excitonic Mott transition [18], i.e., the *dissociation* of the WM excitons, has been predicted based on theoretical considerations on the reduced electron-hole interaction; however, even though the vanishing of absorption peaks has been observed in experiments, the excitonic Mott transition has never been clearly demonstrated for bulk semiconductors with a direct band gap. In addition, the Pauli blocking of the lowest optical transitions is expected to become important and it is believed that an excited electron-hole pair which interacts with the Fermi sea forms a so-called *Mahan exciton*, i.e., a bound state below the quasiparticle (QP) absorption edge [9, 12]. Due to the sharpness of the Fermi surface at low temperatures and Pauli's exclusion principle such Mahan excitons are assumed to cause a Fermi-edge singularity (FES) singularity of the absorption [12]. In a real material, however, the influence of the temperature and the finite lifetime of photo-generated electron-hole pairs broaden the edge anomalies, which is why these many-body effects cannot be observed easily.

In this Letter, we generalize recent theoretical spectroscopy techniques for the calculation of optical properties including excitonic and local-field effects. Our approach is based on the full QP band structure [19] and accomplishes the challenging task of accounting for an additional degenerate electron gas in the lowest CB. Thereby, the Pauli blocking as well as the additional free-carrier contribution to the dielectric screening are included in the calculation of the many-body effects. Our framework captures the involved physics and, in particular, goes beyond previous two-band models that merely relied on the effective-mass approximation [12, 14, 20].

For several years, *ab-initio* calculations based on many-body perturbation theory are able to describe the QP electronic structure as well as the optical properties of non-metals [19]. In order to treat excitonic and optical local-field effects the Bethe-Salpeter equation for the frequency-dependent polarization function P is transformed into an eigenvalue problem for the electron-hole pair Hamiltonian $\hat{H}$ [19]. If the wave-vector dependent occupation numbers $n_V(\mathbf{k})$ and $n_C(\mathbf{k})$ of the

Bloch valence band (VB) $|v\mathbf{k}\rangle$ and CB $|c\mathbf{k}\rangle$ states can take *non-integer* values, $\hat{H}$ reads

$$\hat{H}(cv\mathbf{k},c'v'\mathbf{k}') = \left[\varepsilon_c^{\mathrm{QP}}(\mathbf{k}) - \varepsilon_v^{\mathrm{QP}}(\mathbf{k})\right]\delta_{cc'}\delta_{vv'}\delta_{\mathbf{k}\mathbf{k}'} + \sqrt{|n_c(\mathbf{k}) - n_v(\mathbf{k})|}\Big[-W(cv\mathbf{k},c'v'\mathbf{k}') + 2\bar{v}(cv\mathbf{k},c'v'\mathbf{k}')\Big]\sqrt{|n_{c'}(\mathbf{k}') - n_{v'}(\mathbf{k}')|}. \quad (1)$$

The first summand in Eq. (1) represents the excitation of *non-interacting* quasielectron-quasihole pairs with QP energies $\varepsilon_\nu^{\mathrm{QP}}(\mathbf{k})$, $\nu = \{v,c\}$. Their *interaction* is described by the statically screened Coulomb attraction of the electron and the hole, $-W$, as well as the unscreened exchange-like term for singlet excitations, $2\bar{v}$, to account for the optical local-field effects [19]. The optical absorption coefficient $\alpha_{jj'}(\omega)$ with $j,j' = \{x,y,z\}$ can be derived from the frequency-dependent macroscopic dielectric tensor $\varepsilon_{jj'}(\omega)$ which is obtained from the solution of the eigenvalue problem for $\hat{H}$ [19].

The framework based on this physical picture (cf. Fig. 1a) has successfully been applied in first-principles calculations of optical properties [19–21]. In Fig. 1a the QP energies and the electron-hole pair interaction around the fundamental gap E_g are illustrated for undoped *wz*-ZnO [21] at $T = 0$ K, i.e. for empty CBs ($n_c(\mathbf{k}) = 0$) and occupied VBs ($n_v(\mathbf{k}) = 1$). Additional effects on the QP bands, their occupation, and the electron-hole attraction W have to be taken into account when free carriers are present. Up to free-electron densities of about $5\cdot10^{21}$ cm^{-3}, i.e. for very heavily *n*-doped *wz*-ZnO, the occupation of CB states is restricted to the lowest CB c_0. The free-electron density follows from summing the occupation number $n_{c_0}(\mathbf{k})$ over the entire Brillouin zone, $n = \frac{2}{\Omega_0}\sum_\mathbf{k} n_{c_0}(\mathbf{k})$, with Ω_0 denoting the volume of the unit cell.

First of all, the additional carriers cause an intraband contribution to the electronic polarizability [20] which influences the correlation part of the electronic self-energy and, hence, modifies the QP energies $\varepsilon_\nu^{\mathrm{QP}}(\mathbf{k})$ as well as the screened interaction W. The most important consequence for the QP band structure is the well-known band-gap renormalization (BGR) which leads to $E_\mathrm{g}(n) = E_\mathrm{g} + \Delta E_\mathrm{g}^{\mathrm{BGR}}(n)$ in the doped system [20, 22]. Since the line shape of the absorption coefficient is unaffected by this shift, its discussion is delayed until the results are compared to experiment (cf. Fig. 3).

Second, as illustrated in Fig. 1b and 1d, the electron-hole attraction W is modified due to the electronic intraband polarization caused by the free carriers. Since in (undoped) ZnO the Bohr radius $a_\mathrm{B}^{\mathrm{ZnO}} = 1.8$ nm [8] of the lowest WM-like excitonic bound state is large compared to the characteristic inter-atomic distances, the small-wave-vector limit is used to describe the free-carrier-induced intraband contribution to the screening. Hence, the free-electron-like term $\varepsilon_\mathrm{eff}\bar{q}_\mathrm{TF}^2/q^2$ for the intraband polarizability is added to the background dielectric constant $\varepsilon_\mathrm{eff} = 4.4$, where $\bar{q}_\mathrm{TF}^2$ denotes the Thomas-Fermi wave vector of free electrons in vacuum. Inside a material $\bar{q}_\mathrm{TF}$ is modified by the background screening, i.e. $q_\mathrm{TF} = \bar{q}_\mathrm{TF}/\sqrt{\varepsilon_\mathrm{eff}}$. Adding this intraband contribution to the screening (cf. Fig. 1b) turns the screened Coulomb potential

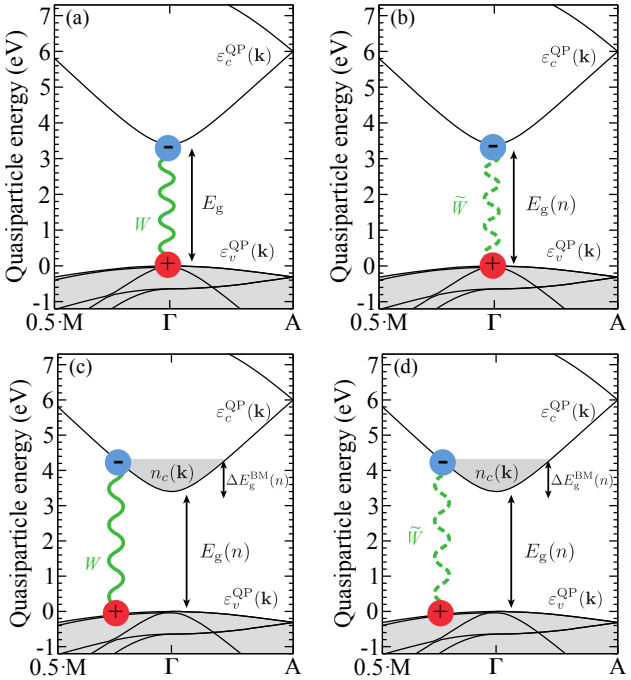

FIG. 1. (Color online) Illustration of free-carrier-induced effects on electron-hole pair excitations near the fundamental band gaps of *wz*-ZnO. (a) Electron-hole interaction (green wavy line) in the undoped material. (b) Additional free-carrier screening affects the electron-hole attraction (dashed green wavy line). (c) Pauli blocking of the lowest CB states causes a Burstein-Moss shift $\Delta E_\mathrm{g}^{\mathrm{BMS}}$ of the absorption edge. (d) Both the Pauli blocking as well as the modified screening affect the formation of excitons.

W in Eq. (1) into a Yukawa-like potential $\tilde{W}$ [23]. This indicates that the degenerate electron gas in the CB reduces the interaction range of the optically induced electron-hole pairs.

Third, the Fermi energy ε_F lies within the (non-parabolic) CB c_0 when a degenerate electron gas is present. The respective occupation number becomes $n_{c_0}(\mathbf{k}) = \Theta\big(\varepsilon_\mathrm{F} - \varepsilon_{c_0}^{\mathrm{QP}}(\mathbf{k})\big)$ in the low-temperature limit. Hence, the lowest CB states around the Γ point in reciprocal space are then occupied (see Fig. 1 and 1d), which is accounted for by the difference of the occupation numbers $n_c(\mathbf{k}) - n_v(\mathbf{k})$ in Eq. (1). This so-called Pauli blocking [20] *prevents* optical transitions into these states. For that reason the optical absorption onset occurs at higher energies; this effect is known as Burstein-Moss shift (BMS). Moreover, since the occupation-number factors in Eq. (1) ensure that only electron-hole pairs contribute to the excitonic Hamiltonian, also the direct influence of the Pauli blocking on the electron-hole interaction is included.

Electronic-structure calculations are carried out using the Vienna *Ab-Initio* Simulation Package (VASP) [24]. The computational approach described in Ref. 21 is pursued. Subsequently, these results are used as input to set up the excitonic Hamiltonian (1). By employing a very fine sampling of the $\mathbf{k}$ space around the pronounced and non-parabolic CB minimum at the Γ point [21, 25] free-electron densities of $n \approx 10^{17}$ cm^{-3} can be resolved. The lowest eigenvalues and eigenstates of

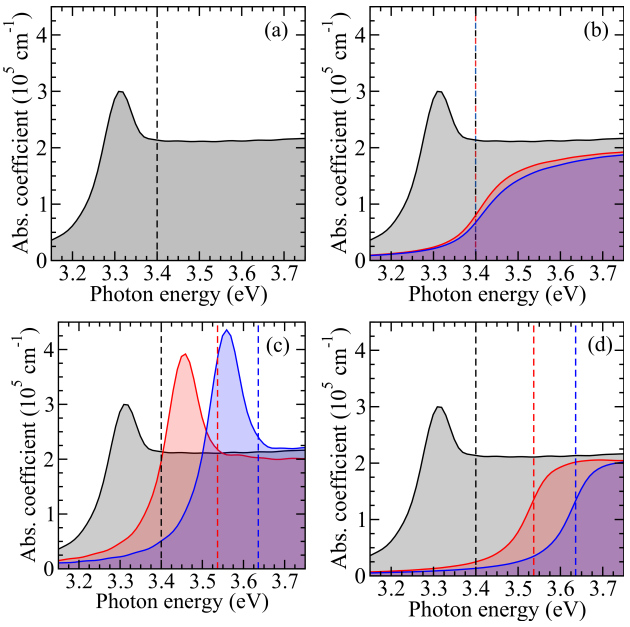

FIG. 2. (Color online) The absorption coeff cient of ZnO is plotted versus photon energy for ordinary light polarization. The situation without doping (black curves) in (a) is compared to spectra calculated for free-electron concentrations of $n = 1.9 \cdot 10^{19}$ cm^{-3} (red) and $n = 4.8 \cdot 10^{19}$ cm^{-3} (blue). In (b) the intraband screening due to the free electrons is taken into account. The inf uence of the Pauli blocking is depicted in (c), and in (d) both effects are included. The respective quasiparticle absorption edges (increased by the Burstein-Moss shift) are indicated by vertical dashed lines.

the excitonic Hamiltonian are obtained via iterative diagonalization [25] and the frequency-dependent dielectric function is calculated by means of an eff cient time-evolution scheme [26]. To account for f nite temperatures and a f nite lifetime of the excited electron-hole pairs, as well as a limited instrumental resolution, a Lorentzian broadening of $\gamma = 50$ meV is assumed for the absorption spectra.

As can be seen in Fig. 2a the absorption onset of undoped ZnO is dominated by bound excitonic states. The width and the shape of the peak structure in the absorption spectrum below the fundamental band gap emerge from two underlying WM-like exciton series [10, 11]. Even though above E_g only scattering states of the excitons occur, the spectrum is still strongly affected by excitonic effects due to the Coulomb enhancement [11, 20].

In order to disentangle the effects that arise from the modif ed electron-hole attraction $\tilde{W}$ and the Pauli blocking they are included separately in the calculations f rst, before all free-carrier-induced effects are combined. In a f rst step, the impact of the free carriers on the screened electron-hole attraction is taken into account ($W \to \tilde{W}$). The optical-absorption curves in Fig. 2b illustrate that the binding energies and oscillator strengths of the band-edge excitons are more and more reduced due to the smaller interaction range of the electrons and holes. While the absorption edge starts to resemble the one of non-interacting electron-hole pairs, the inf uence of the additional screening due to the free electrons is less pronounced for higher photon energies (cf. Fig. 2b).

The observation that bound excitonic states seem to vanish for high doping levels can be an indication for a Mott transition of the lowest electron-hole pairs. Many numerical works (see e.g. Ref. 27 and references therein) investigated a model Hamiltonian consisting of a parabolic kinetic energy term and a Yukawa potential, f nding that it has no bound states for inverse screening lengths q_{TF} that fulf ll the Mott criterion $q_{TF} \cdot a_B > 1.19$. Using ε_{eff} this relation yields a Mott density of $n_M = 5.94 \cdot 10^{18}$ cm^{-3} for which the excitonic Mott transition occurs in ZnO. The curves in Fig. 2b, calculated for two typical free-electron concentrations of $n = 1.9 \cdot 10^{19}$ cm^{-3} and $n = 4.8 \cdot 10^{19}$ cm^{-3}, support this picture, since the pronounced excitonic peak disappears. However, that is not the whole truth.

In contrast to Fig. 2b, in Fig. 2c solely the Pauli blocking is taken into account; this shifts the absorption onset towards higher photon energies in n-doped ZnO. More precisely, $\Delta E_g^{BMS}(n = 1.9 \cdot 10^{19}\,\text{cm}^{-3}) = 0.137$ eV and $\Delta E_g^{BMS}(n = 4.8 \cdot 10^{19}\,\text{cm}^{-3}) = 0.236$ eV is derived from the QP band structure. In addition, Fig. 2c indicates that for increasing free-electron concentrations bound excitonic states persist below the QP band edge (including BMS), i.e. below $E_g + \Delta E_g^{BMS}(n)$. The increase of the height of the corresponding peaks with increasing n, which contradicts both physical intuition as well as experimental f ndings [9], is related to the pronounced FES [12] at the absorption onset. When the free-carrier screening is neglected, the FES arises from the growing Fermi surface and the modif cation of the effective electron-hole attraction by the occupation-number factor in Eq. (1).

Accounting simultaneously for the Pauli blocking and the additional screening term leads to the absorption coeff cients shown in Fig. 2d. The increase of the oscillator strength observed in Fig. 2c is counteracted by the intraband screening contribution. Comparing Fig. 2d to Fig. 2b reveals that the full approach yields Mahan-exciton-like features [12] at the absorption edge. As shown below in Fig. 3, they arise from bound excitonic states which affect the absorption line shape also when the exciton binding energies are negligibly small. However, due to lifetime, temperature, and instrumental broadening, the Fermi edge and the accompanying singularities are smeared out; hence, in praxis the bound states do not appear as distinct peaks in Fig. 2d. The resulting similarity of the curves in Fig. 2b and 2d explains why it is diff cult to distinguish between the formation of Mahan excitons and a Mott transition by looking at absorption spectra.

In the literature the Mott density is heavily debated; much smaller or much larger values than $n_M = 5.94 \cdot 10^{18}$ cm^{-3} have been derived from measured spectra [8]. To enlighten this issue, the binding energy of the lowest excitonic bound state for the doped system along with the corresponding oscillator strength is given in Fig. 3a. A rapid decrease of both by orders of magnitude with an increasing density n of the degenerate electron gas is evident. Nevertheless, excitonic states with binding energies of up to 2 meV and oscillator strengths as

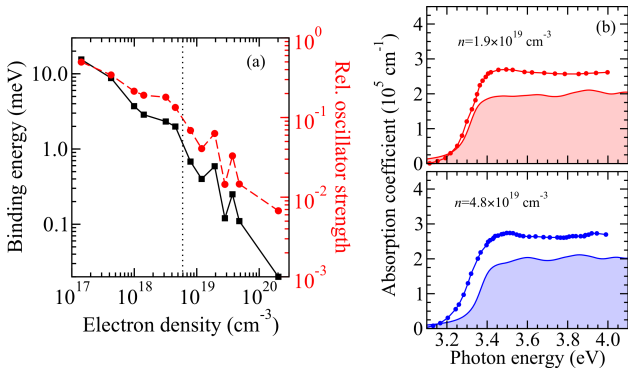

FIG. 3. (Color online) Calculated optical absorption coeff cients (solid lines) of *n*-doped ZnO for ordinary light polarization, with (a) $n = 1.9 \cdot 10^{19}$ cm^{-3} (red) or (b) $n = 4.8 \cdot 10^{19}$ cm^{-3} (blue). Measured curves (solid lines with dots) are taken from Ref. 9. (c) Exciton binding energy (solid) and relative oscillator strength (dashed), normalized with respect to the oscillator strength of the A exciton of undoped ZnO, versus free-electron concentration n. The dotted line indicates the density n_{M} calculated from the Mott criterion (see text). The f uctuations within $\lesssim 1$ meV arise due to the numerical accuracy.

large as 7 % of the value for the lowest bound WM-like state in the undoped material still exist for electron densities *larger* than the nominal Mott density n_{M}. Hence, no excitonic Mott transition occurs when the full QP band structure, the additional intraband screening, and the Pauli blocking are consistently taken into account. Instead, these states are attributed to Mahan excitons. Mahan found for a two-band model [12] that the binding energy only vanishes for $n \to \infty$. However, since the decrease is continuous and the inf uence of broadening effects is large, the behavior depicted in Fig. 3a can readily be mistaken as a Mott transition of the exciton.

The aforementioned *intra*band contribution to the electronic polarizability caused by the additional electrons is small compared to the *inter*band screening due to the valence electrons. Hence, its exact treatment within the *GW* framework is of minor importance. In order to still account for the BGR when comparing the calculated absorption spectra to measured ones, a Lindhard-like description of the intraband polarization is suff cient [22]. The approximate shifts $\Delta E_{\mathrm{g}}^{\mathrm{BGR}}(n = 1.9 \cdot 10^{19}\ \mathrm{cm}^{-3}) = -0.213$ eV and $\Delta E_{\mathrm{g}}^{\mathrm{BGR}}(n = 4.8 \cdot 10^{19}\ \mathrm{cm}^{-3}) = -0.261$ eV were taken into account for the following discussion of the absorption spectra depicted in Fig. 3b.

Comparing the calculated absorption coeff cients to results measured for highly Al-doped ZnO [9] shows very good agreement regarding the energetic position as well as the line shape of the absorption edge (Fig. 3b). The absolute position of the onset and its small variation [9] for different doping levels can be explained by a blueshift (due to the BMS) and a redshift (due to the BGR) that largely compensate each other for $n = 1.9 \cdot 10^{19} \ldots 4.8 \cdot 10^{19}$ cm^{-3}. Having merely used a model [22] to calculate the BGR most likely explains the difference of less than 50 meV between the measured and the calculated position of the absorption onset for $n = 4.8 \cdot 10^{19}$ cm^{-3}. Overall, Fig. 3b impressively points out that accounting simultaneously for all relevant many-body effects in the calculations yields an unprecedented agreement of the absolute values of the frequency-dependent absorption coeff cient with curves measured for doped ZnO. Thereby, any inter-conduction-band absorption is found to be negligible for $n \lesssim 10^{21}$ cm^{-3}.

In this work, the band-gap renormalization, the Pauli blocking of optical transitions, the reduction of the electron-hole attraction, and the occupation-induced modif cations of the electron-hole interaction have been taken into account simultaneously for the f rst-principles calculation of the frequency-dependent absorption coeff cient of *n*-ZnO. By disentangling the different many-body effects, this work paves the way to a deep, quantitative understanding of the intricate interplay of excitons and doping in TCOs. An excellent agreement with experimental results proves that our framework captures the involved physics. Finding no complete dissociation of the lowest bound excitonic state shows that no Mott transition of the exciton occurs; instead, a Mahan-like exciton evolves in the doped system. The approach is readily applicable to other highly doped non-metals and can easily be extended towards *p*-doped systems.

We acknowledge discussions with R. Goldhahn, P. Rinke, A. Janotti, and C. G. Van de Walle. Financial support by the European Community within the e-I3 project ETSF (GA No. 211956) and the Deutsche Forschungsgemeinschaft (Project No. Be 1346/20-1) is acknowledged. A. S. thanks the Carl-Zeiss-Stiftung and Heptagon for support. Part of this work was performed under the auspices of the U.S. Department of Energy at Lawrence Livermore National Laboratory under Contract DE-AC52-07NA27344.

* a.schleife@llnl.gov

[1] M. Law, L. E. Greene, J. C. Johnson, R. Saykally, and P. Yang, Nature Materials **4**, 455 (2005).
[2] K. Nomura, H. Ohta, A. Takagi, T. Kamiya, M. Hirano, and H. Hosono, Nature **432**, 488 (2004).
[3] A. P. Ramirez, Science **315**, 1377 (2007).
[4] Y. Qin, X. Wang, and Z. L. Wang, Nature **451**, 809 (2008).
[5] E. Comini and G. Sberveglieri, Mater. Today **13**, 36 (2010).
[6] H. Hosono, in *Handbook of Transparent Conductors*, edited by D. S. Ginley (Springer, 2010) pp. 459–487.
[7] U. Özgür, Y. I. Alivov, C. Liu, A. Teke, M. A. Reshchikov, S. Doğan, V. Avrutin, S.-J. Cho, and H. Morkoç, J. Appl. Phys. **98**, 041301 (2005).
[8] C. Klingshirn, R. Hauschild, J. Fallert, and H. Kalt, Phys. Rev. B **75**, 115203 (2007).
[9] T. Makino, K. Tamura, C. H. Chia, Y. Segawa, M. Kawasaki, A. Ohtomo, and H. Koinuma, Phys. Rev. B **65**, 121201 (2002).
[10] A. Schleife, C. Rödl, F. Fuchs, J. Furthmüller, and F. Bechstedt, Appl. Phys. Lett. **91**, 241915 (2007).
[11] R. J. Elliott, Phys. Rev. **108**, 1384 (1957).
[12] G. D. Mahan, Phys. Rev. **153**, 882 (1967).
[13] M. Combescot and P. Nozières, J. Phys. France **32**, 913 (1971).
[14] P. Hawrylak, Phys. Rev. B **44**, 3821 (1991).
[15] V. Huard, R. T. Cox, K. Saminadayar, A. Arnoult, and

S. Tatarenko, Phys. Rev. Lett. **84**, 187 (2000).
[16] M. Feneberg, J. Däubler, K. Thonke, R. Sauer, P. Schley, and R. Goldhahn, Phys. Rev. B **77**, 245207 (2008).
[17] F. Fuchs, K. Kheng, P. Koidl, and K. Schwarz, Phys. Rev. B **48**, 7884 (1993).
[18] N. F. Mott, *Metal-Insulator Transitions* (Taylor & Francis, London, 1990).
[19] G. Onida, L. Reining, and A. Rubio, Rev. Mod. Phys. **74**, 601 (2002).
[20] S. Glutsch, *Excitons in Low-Dimensional Semiconductors: Theory, Numerical Methods, Applications* (Springer, 2004).
[21] A. Schleife, C. Rödl, F. Fuchs, J. Furthmüller, and F. Bechstedt, Phys. Rev. B **80**, 035112 (2009).
[22] K. F. Berggren and B. E. Sernelius, Phys. Rev. B **24**, 1971 (1981).
[23] H. Yukawa, Proc. Phys. Math. Soc. Jap. **17**, 48 (1935).
[24] G. Kresse and D. Joubert, Phys. Rev. B **59**, 1758 (1999).
[25] F. Fuchs, C. Rödl, A. Schleife, and F. Bechstedt, Phys. Rev. B **78**, 085103 (2008).
[26] W. G. Schmidt, S. Glutsch, P. H. Hahn, and F. Bechstedt, Phys. Rev. B **67**, 085307 (2003).
[27] Y. Li, X. Luo, and H. Kröger, Sci. China Ser. G **49**, 60 (2006).